A novel surgical technique for a rat subcutaneous implantation of a tissue engineered scaffold

Reza Khorramirouz, **Jason L. Go**, **Christopher Noble**, **Soumen Jana**, **Eva Maxson**, **Amir Lerman**, **Melissa D. Young**[*]

Department of Cardiovascular Medicine, Mayo Clinic, Rochester, MN, United States

Abstract

Objectives—Subcutaneous implantations in small animal models are currently required for preclinical studies of acellular tissue to evaluate biocompatibility, including host recellularization and immunogenic reactivity.

Methods—Three rat subcutaneous implantation methods were evaluated in six Sprague Dawley rats. An acellular xenograft made from porcine pericardium was used as the tissue-scaffold. Three implantation methods were performed; 1) Suture method is where a tissue-scaffold was implanted by suturing its border to the external oblique muscle, 2) Control method is where a tissue-scaffold was implanted without any suturing or support, 3) Frame method is where a tissue-scaffold was attached to a circular frame composed of polycaprolactone (PCL) biomaterial and placed subcutaneously. After 1 and 4 weeks, tissue-scaffolds were explanted and evaluated by hematoxylin and eosin (H&E), Masson's trichrome, Picrosirius Red, transmission electron microscopy (TEM), immunohistochemistry, and mechanical testing.

Results—Macroscopically, tissue-scaffold degradation with the suture method and tissue-scaffold folding with the control method were observed after 4 weeks. In comparison, the frame method demonstrated intact tissue scaffolds after 4 weeks. H&E staining showed progressive cell repopulation over the course of the experiment in all groups with acute and chronic inflammation observed in suture and control methods throughout the duration of the study. Immunohistochemistry quantification of CD3, CD 31, CD 34, CD 163, and αSMA showed a statistically significant differences between the suture, control and frame methods ($P < 0.05$) at both time points. The average tensile strength was 4.03 ± 0.49, 7.45 ± 0.49 and 5.72 ± 1.34 (MPa) after 1 week and 0.55 ± 0.26, 0.12 ± 0.03 and 0.41 ± 0.32 (MPa) after 4 weeks in the suture, control, and frame methods; respectively. TEM analysis showed an increase in inflammatory cells in both suture and control methods following implantation.

Conclusion—Rat subcutaneous implantation with the frame method was performed with success and ease. The surgical approach used for the frame technique was found to be the best methodology for *in vivo* evaluation of tissue engineered acellular scaffolds, where the frame method did not compromise mechanical strength, but it reduced inflammation significantly.

[*]Corresponding author at: 200 First St SW, Rochester, MN 55905, United States. Young.Melissa@mayo.edu (M.D. Young).

Conflict of interest

There are no financial interests or relationships with industry associated with this paper.

1. Introduction

Certain aspects of tissue response to biomaterials are important from research and development perspectives. The *in vivo* evaluation of tissue reaction to these materials is important for performance, safety, and regulatory reasons. The International Organization of Standardization and the Food and Drug Administration (FDA) indicate the required tests needed for the introduction of different biocompatible tissues (Anderson, 2001). During the early stages of development, *in vivo* evaluation provides researchers insight to the proposed manufacturing processes and design of tissue engineered scaffolds. Additionally, these tests should be repeated with the final manufacturing and sterilization conditions found in the final product.

Currently, subcutaneous implantation in small animal models are used for preclinical testing to evaluate immune reactivity and recellularization capacity (Neethling et al., 2010; Rennert et al., 2013; Sarkanen et al., 2012). Although it is common to use different animals such as rabbits and mice for subcutaneous implantation; rat subcutaneous implants are one of the most studied because it enables the assessment of tissue compatibility such as possible sensitization, irritation, intracutaneous reactivity, systemic toxicity, genotoxicity, implantation, chronic toxicity, carcinogenicity, biodegradation, and immune response (Modulevsky et al., 2016; Wang et al., 2017; Cunniffe et al., 2015; Ripamonti, 1996). Despite time and costs, it is crucial to have a reliable method for implantation. Subcutaneous implantation allows for the observation of an inflammatory response, cellularization of the extracellular matrix, and angiogenesis validation (Modulevsky et al., 2016; Guarnieri et al., 2014; Stapleton et al., 2010; Meagher et al., 2016; Mazza et al., 2015).

Various scaffolds have been explored with a subcutaneous model of implantation such as Polylactides (PLA), poly(3-hydroxybutyrate), porcine small intestine submucosa, and bioengineered acellular scaffolds (Gogolewski et al., 1993; Zheng et al., 2005; Yang et al., 2008; Nillesen et al., 2007). Most studies use the same technique for subcutaneous implantation by placing the biomaterial under the skin without fixation (Kim et al., 2007). The current study suggests that the method of subcutaneous implantation could affect recellularization and inflammatory outcomes (Setzen and Williams, 1997). Therefore, it is crucial to have a stringent methodology that will minimize tissue degradation in the host, while minimizing inflammation and maximizing the recellularization capacity. We hypothesize that application of a PCL composed frame as a support for an acellular scaffold will provide better outcomes in the subcutaneous location of a rat reducing inflammation and better biomechanical properties.

2. Materials and methods

2.1. Procurement, decellularization, and sterilization of porcine pericardium

Freshly harvested porcine pericardium was obtained from a local abattoir (Hormel Food Corporation, USA). The tissue was stripped of adjacent fat and rinsed with phosphate buffered saline solution (PBS). The tissue was processed with sodium dodecyl sulfate (SDS), DNase, and diH$_2$O with constant agitation for 2 days at room temperature. An additional exposure and wash with DNase, Tris buffer, MgCl$_2$, peroxyacetic acid (PAA), and phosphate buffered solution (PBS) was performed. The decellularized pericardial tissue was sterilized using supercritical carbon dioxide (NovaSterilis, Inc., USA). The detailed decellularization and sterilization process parameters are outlined in our previous work (Hennessy et al., 2017).

2.2. Biomaterial frame composition

The frame-like structures used to support the implanted tissue were 3D-printed using an Envision TEC 3D-Bioplotter. The 3D computer aided drawing (CAD) model of the ring was generated, with an inner and outer diameter of 19.2 mm and 22.7 mm, respectively. The CAD model was uploaded to the Magics Envision TEC software (32 bit, version 16.2.0.20, Materialize n.v. 2011) where it was modified before being uploaded to the Bioplotter software (version 3.0.713.1406, Envision TEC), which enables slicing of the model, before 3D-printing. The slice thickness utilized was 320 μm. The resulting file was uploaded to the software Visual Machines (version 2.8.126) that allows the user to input the various parameters that control the bioprinter. Polycaprolactone (PCL, Mn 45,000, and Sigma-Aldrich) beads were loaded into the high temperature stainless-steel cartridge and heated to 130 °C for 2 h. The rings were printed onto an inverted 120 mm diameter glass petri dish (Duroplan, Germany) that was stabilized by a petri dish holder. Nine rings were printed at a time, side-by-side, each made of one extruded layer of PCL. The strands of PCL were printed 0.4 mm apart, with a needle vertical offset of 0.05 mm and using a stainless steel needle of 0.7 mm inner diameter. The printing platform temperature was kept at 35 °C, and the cartridge at 130 °C throughout the printing process, the speed and extrusion pressure were set to be 2.3 mm/s and 6 bar, respectively. Reproducibility of the PCL support frames was ensured by using the same CAD model for each frame, and by the high XYZ axis resolution of the Bioplotter (0.001 mm).

2.3. Surgical implantation

Six Sprague Dawley rats were obtained and were raised in a pathogen-free environment throughout the experiment. All experiments were performed in strict accordance with the recommendations in the Guide for Institutional Animal Care and Use Committee (protocol number: A00001864-16). The rats were classified into 3 groups with different surgical implantation methods, 2 rats for each method produced a total of 8 specimens per group. The rats were induced by isoflurane 4% and maintenance of 2% and shaved, and then the buprenorphine (0.6 mg/kg) was injected subcutaneously. The animals were positioned in prone to provide better oxygenation. After scrubbing with betadine, the 20 mm dorsal midline incision was made over the thoracolumbar area. Two tissue scaffolds were inserted at both sides. The adjacent fascia was released and three surgical methods were applied:

Method 1 (suture): The acellular porcine pericardium was cut into 20 mm × 20 mm segments and placed over the muscle under the skin and the scaffold was sutured at four corners with Polypropylene 5-0.

Method 2 (control): The scaffold was cut the same as above and placed subcutaneously without suturing and fixation.

Method 3 (frame): The scaffold was fixed to the PCL rim frame by Polypropylene 5-0 under sterile conditions. Then the fixed scaffold was placed between skin and fascia and left in position.

All the animals were closed with Vicryl 4-0 and received topical tetracycline and followed-up for 1 and 4 weeks post-implantation.

2.4. Histology and immunohistochemistry

After 1 and 4 weeks, tissue samples were biopsied, sectioned, and paraffin-embedded. The samples underwent Hematoxylin-Eosin (H&E), Masson's trichrome, and Picrosirius red staining per manufacturer's protocol. Recellularization and immune reaction were evaluated using immunohistochemistry with various antibodies. Recellularization of endothelial-like and interstitial-like cells was evaluated using CD 34 (Abcam, Cambridge, UK), CD 31(Abbiotec, San Diego, CA), alpha smooth muscle actin (Sigma, St. Louis, MO), and vimentin (Abcam, Cambridge, UK) while immune reaction was evaluated using CD 168 (Abcam, Cambridge, UK) and CD 3 (Abcam, Cambridge, UK) antibodies. Tissue samples were labeled with the Dako Envision System-HRP, blocked with the Dako peroxidase solution incubated in primary antibody overnight at 4 °C with the secondary antibody (biotinylated rabbit anti-rabbit Ig F [ab'] 2 fragments; Dako). All the images were captured using 10× and 20× magnification by light microscopy. All images were analyzed using Image J software, which was previously determined to be a validated method (Vogel et al., 2016). Quantitative assessment of Picrosirius staining was done by capturing 8 images in different regions across the tissue sample. The stained area was measured and presented as percent area. For DAPI staining the same procedure was done and cell signaling was counted per area and reported as percent area. For immunohistochemistry the positive stained area was measured.

2.5. Transmission electron microscopy

Tissues were fixed in Trumps fixative at 4 °C overnight per manufacturer's protocol. These were then washed in PBS, rinsed in water, fixed in 1% osmium tetroxide (OsO4), dehydrated through a graded series of ethanol, and embedded in Spur resin. Ultra-thin sections (100 nm or 0.1 μm) were cut and mounted on 200-mesh copper grids. After being post-stained with lead citrate, they were imaged in a JEOL (JEM-1400 Plus) transmission electron microscope.

2.6. Biomechanical properties: uniaxial mechanical testing

The biomechanical properties were evaluated at 1 and 4 weeks for all 3 methods. The testing was conducted on 4 samples with each group, for a total of 24 samples. The uniaxial tensile testing was performed with a tensile tester (Instron, USA). Each tissue specimen was cut

into 4 equal pieces with dimensions of 12 mm × 5 mm. The thickness was measured with a thickness gauge (Mitutoyo, Japan) and recorded for each sample. The sample was placed between the grips. Test samples were loaded at the extension rate 0.1 mm/s and elongated until failure. Extension versus load data were recorded and used to calculate the ultimate tensile strength. Engineering stress was calculated by dividing the measured force by the initial cross sectional area and strain by dividing the measured displacement by the initial sample length. Maximum tensile stress and tangent modulus in the linear region were used to compare mechanical responses.

2.7. Explanation and biopsy

The animals were sacrificed after 1 and 4 weeks post implantation. The rats were euthanized with 10% CO_2 chamber for 5 min. The animals were shaved and a dorsal midline incision was made. The adjacent fascia was released by gentle dissection to find the explanted tissue.

2.8. Statistical analysis

Data distribution was analyzed utilizing MATLAB statistics toolbox, comparisons between explant times were analyzed using a Student's unpaired *t*-test. While comparison between implantation methods was performed using a one way ANOVA followed by a multi-comparison test. Data is presented as means ± SD with statistical significance defined as *P* value < 0.05.

3. Results

3.1. Macroscopic findings

All animals survived the procedure with no evidence of sepsis or infection. There were different macroscopic findings between groups (Fig. 1). In method 1 (suture method), the scaffold integrated into host tissue which separated with difficulty from the host tissue after 1 week. After 4 weeks part of the tissue completely degraded into host tissue, which was again difficult to remove from host tissue. Method 2 (control method) had no integration, but the tissue was folded completely on top of itself with shrinkage after 1 and 4 weeks. For method 3 (frame method) the scaffold was easily identified with no evidence of degradation and folding into the host tissue.

3.2. Histopathological evaluation

Hematoxylin and eosin staining showed cellular infiltration in suture and non-suture methods (Fig. 2). Increased levels of new vessel formation surrounding the inflammatory cells were seen after 1 week in both suture and non-suture methods. In contrast the tissues implanted with the frame method are free of inflammatory cells and progressively infiltrated by host cells. After 4 weeks, DAPI staining showed increased recellularization between all the groups (13.99 ± 0.33, 15.13 ± 0.93 and 4.37 ± 0.19 in suture, control, and frame methods) (Fig. 2). The inflammatory reaction was also present after 4 weeks in both suture and control methods which are predominantly observed as chronic infiltration. In contrast, the frame method had no infiltration of inflammatory cells at 4 weeks. Picrosirius staining and collagen content had a change in distribution with time (Fig. 3). After 1 week the collagen fiber concentration was 68.45 ± 2.76, 70.56 ± 1.45 and 73.45 ± 2.99 in suture,

control, and frame methods, respectively. Compared to 4 weeks the collagen content and distribution decreased significantly in all the groups (43.29 ± 1.70, 40.34 ± 1.52 and 45.56 ± 5.93). Table 1 shows the statistical comparison of collagen content from picrosirius red staining. Comparing between implantation methods at weeks 1 and 4 no differences are statistically significant.

3.3. Transmission electron microscopy

Analysis of implantation techniques after 1 week showed increased neutrophil and lymphocytic infiltration in the suture and control methods. The frame method showed collagen fiber with few host cells seeded on the scaffold at both 1 and 4 weeks. After 4 weeks, macrophage infiltration was detected in the suture method. In the control method, there was a high level of cellular infiltration, which is characteristic of chronic inflammation (Fig. 4).

3.4. Biomechanical properties

After 1 week post implantation, maximal tensile stress was 4.03 ± 0.49 MPa, 7.45 ± 0.49 MPa, and 5.72 ± 1.34 MPa in the suture, control, and frame methods, respectively. The calculated tangent modulus was 16.09 ± 2.61 MPa, 30.98 ± 10.25 MPa, and 25.19 ± 11.07 MPa in the suture, control, and frame methods. The maximum tensile stress after 4 weeks was 0.55 ± 0.26 MPa, 0.12 ± 0.03 MPa, and 0.41 ± 0.32 MPa for the suture, control, and frame methods; respectively. While the tangent modulus was 2.38 ± 0.66 MPa, 0.36 ± 0.12 MPa, and 1.48 ± 1.13 MPa for the suture, control, and frame methods (Fig. 5). There was a statistical significant difference between control and suture methods for tensile stress at week 1 (Table 2).

3.5. Immunohistochemistry

Immunohistochemistry was performed for the entire scaffold at 1 and 4 weeks. The CD 3 staining showed highly positive inflammatory cells in both the suture (3.52 ± 0.82) and control methods (8.95 ± 1.28) especially at 1 week compared to the frame method (0.09 ± 0.01) Fig. 6. At 4 weeks, there was a marked increase in CD 3 staining for the suture and control method (21.76 ± 0.27 and 15.12 ± 0.13; respectively) compared to the frame method (0.18 ± 0.03) (Fig. 7). Specific staining for macrophage type 2 (CD 163) revealed very weak staining after 1 week (0.26 ± 0.03, 0.7 ± 0.13 and 0.06 ± 0.02 in suture, control, and frame methods; respectively). At 4 weeks there was a marked increase in all methods for CD 163 staining (7.15 ± 0.14, 4.18 ± 0.03 and 7.4 ± 0.15 in suture, control, and frame methods; respectively) (Fig. 7). Angiogenesis markers CD 31 and CD 34 showed highly positive staining in the control and suture methods at 1 week (5.6 ± 0.58 and 8.03 ± 0.41 suture and control methods for CD 31; 1.7 ± 0.62 and 3.5 ± 0.29 for CD 34) (Fig. 8). The frame method showed a progressive increase in both CD 31 and CD 34 overtime (1.6 ± 0.15 and 0.91 ± 0.13 for CD 31 and CD 34 at 1 week; versus 3.5 ± 0.25 and 2.92 ± 0.25 for CD 31 and CD 34 at 4 weeks), Fig. 9. Alpha-smooth muscle actin (α-SMA) was observed to be highly expressed after 4 weeks in both the control and suture methods (Fig. 10). This infiltration is indicative of recellularization of myofibroblast-like interstitial cells that determine functionality of the tissue, which includes new collagen formation. Vimentin staining showed highly positive staining in all methods after 4 weeks (6.8 ± 0.12, $6.9 \pm$

0.15 and 2.9 ± 0.4 for suture, control, and frame methods), but weak staining at 1 week (0.4 ± 0.15, 0.3 ± 0.3 and 0.14 ± 0.04 for suture, control and frame method) (Fig. 11). Comparing between implantation methods at weeks 1 and 4 both suture and frame methods were statistically significant compared to controls for semi-quantitative analysis of all stains bar Vimentin where only the frame method was significant (Table 3). In addition, when comparing the suture method to the frame method, results were significant for Vimentin at week 1.

4. Discussion

This study characterizes several different techniques of subcutaneous implantation for a tissue-engineered scaffold. Key outcomes such as tissue degradation, biomechanical properties, inflammation, and recellularization were analyzed for each method. Evaluating different surgical methods is significant because there is a need to evaluate biocompatibility prior to *in vivo* implantation of surgical devices (Sarkanen et al., 2012; Wu et al., 2016; Lai et al., 2005; Costa et al., 2005; Tran et al., 2016; Mirsadraee et al., 2007; Wang et al., 2005). However, an inadequate approach to implantation could interfere with the tissue engineered scaffold causing problems with recellularization. A gold standard technique for subcutaneous implantation is imperative for reliable results. To adequately access biocompatibility there are a few concerns regarding implantation such as degradation and inflammation (Record et al., 2001; Zhang et al., 2011; Badylak et al., 1998). Three methods of subcutaneous implantation were evaluated on acellular porcine pericardium at 1 and 4 weeks. It was determined that surgical techniques may have an affect with biocompatibility responses.

Macroscopic evaluation showed an intact structure for samples prepared with the frame method compared to the suture and control methods. Tissue degradation was observed for the suture method after 1 month, where the tissue was found to be integrated into the host tissue. This integration may be explained by fixation of the scaffold with adjacent muscle. Badylak et al. observed that tissue engineered scaffolds made from naturally derived small intestinal submucosa underwent rapid and complete degradation (Record et al., 2001). Zhang et al. implanted porcine small intestine submucosa (SIS) and showed shrinkage compared to a growth seen in pericardial and dermal matrix tissues after 8 weeks post implantation (Zhang et al., 2011). The degradation phenomenon was not limited to SIS, but also in pericardium after subcutaneous implantation in a rat aorta which showed degradation after implantation (Walles et al., 2003). Tissue degradation happens when the scaffold disappears or is reabsorbed into the host. Badylak et al. proposed that tissue degradation could be the result of repopulation of implanted acellular tissue with host cells. It was hypothesized that the biomaterial was rapidly degraded and replaced by host tissue that became organized and differentiated similarly to urinary bladder tissue (Record et al., 2001; Badylak et al., 1998).

The control method showed scaffold folding in both 1 and 4 weeks after implantation which was due to lack of tissue support. The tissue folding caused shrinkage by 30%. The frame method kept the scaffold intact with no degradation into the host tissue making it easier to dissect by adjacent fascia. Additionally, due to fixation of tissue to the frame, there was no

observed tissue folding, and macroscopic evaluation confirmed the advantage of the frame technique over the suture and control methods.

When comparing the mechanical response between the different implantation methods after 1 week, the control method had increased stiffness and tensile stress. The suture method showed significantly lower mean tensile stress and stiffness when compared to the other implantation methods; however, after 4 weeks, it had the highest mean tensile stress and stiffness. Additionally after 4 weeks, the control method showed the lowest stiffness and tensile stress, which may be explained through tissue folding and shrinkage. Across the two explant times, both the frame and suture methods consistently showed the most desirable mechanical response. It may be explained that the difference between 1 and 4 weeks with all methods is that the scaffold was infiltrated with host cells that was replaced with transplanted tissue causing deterioration of the biomechanical properties. Tohyama et al. suggested that cell infiltration and angiogenesis from adjacent tissues may be responsible for the deterioration of mechanical properties found in the patellar tendon matrix after implantation. Another plausible explanation may be related to the scaffold thickness that increased from 25 mm to 70 mm after 4 weeks implantation. The thickness inversely impacts the biomechanical properties as a thick scaffold would require an increased force to give the same value of tensile stress. Extrinsic cellular infiltration by the host tissue increases the scaffold thickness, but perhaps as primary pericardial architecture. The biomechanical properties from the explanted tissues in all three implantation methods decreased due to infiltration of the extrinsic cells into the scaffold. This finding was supported by Zhang et al. which demonstrated that the median tensile strength of porcine pericardium decreased 4 weeks after abdominal wall reconstruction in a rat model (Zhang et al., 2011).

In the suture method, increased inflammation was observed to be distributed over the scaffold. Andrade et al. suggested that the tissue reaction to suture materials depend mainly on polymer composition and suture materials induced differentiated tissue reactions (Andrade et al., 2006). Katz et al. hypothesized that the chemical composition of the suture material plays an important role in the interaction between bacteria and suture that is a determinant of severity and persistent of tissue infection (Katz et al., 1981). Another study mentioned high levels of neutrophil, macrophage infiltration and foreign body reaction after 4 days in the site of retention suture (Ascherman et al., 2005). Sencan et al. also reported inflammatory reaction to suture materials with their tissue, where tissue fixed with silk and polypropylene caused more inflammation and destruction of somniferous tubular compared with fibrin glue (encan et al., 2004). The Petrut findings showed suture material in the bladder supported intense and moderate tissue reaction with monofilament and Vicryl after 3 weeks respectively (encan et al., 2004). A notable finding was the increased inflammatory reaction in the control method, specifically in the folded area. This demonstrates that tissue shrinkage and folding may contribute to recruitment of inflammatory cells. The frame methods resulted in the least inflammation due to lack of suture material and the elimination of any folded tissue.

The composition of the frame itself is very important since there are many biomaterials used previously and different inflammatory responses were reported. PCL is highly suitable for

in vivo implantation because of its slower degradation rate compared to other biomaterials like polyglycolide (PGA), and poly d, l-lactide (PDLA). Woodruff et al. mentioned it takes 2–4 years for PCL to degrades (Thiel et al., 2005). Kristy et al. reported PCL had the least inflammatory reaction between the biomaterials used in their study (Ainslie et al., 2009). Sun et al. reported that *in vivo* degradation of PCL was observed for 3 years in rats (Sun et al., 2006). Another study evaluated *in vivo* implantation of Nano-D400G and Nano-PCL revealed higher vascular density and less inflammation after 4 weeks in Nano PCL (Giavaresi et al., 2006). The PCL has some preference in the terms of recellularization, where Singh et al. found an increase in angiogenesis and vasculogenesis in heparin-PCL scaffolds seeded by endothelial progenitor cells after 1 week (Singh et al., 2011).

Application of a support frame during implantation of a tissue engineered scaffold is critical for keeping the tissue intact and obtaining accurate biomechanical properties. Both suture and frame methods preserved the biomechanical properties; however, the frame method had other preferential factors such as less recruitment of inflammatory cells.

5. Conclusion

We demonstrated that different surgical techniques for rat subcutaneous implantation could affect the *in vivo* results of tissue engineered scaffolds such as acellular porcine tissue. Application of a frame composed of PCL fibers were found to be an effective and supportive structure to hold the scaffold in position, prevent degradation, and decrease inflammation compared to traditional methods.

Supplementary Material

Refer to Web version on PubMed Central for supplementary material.

Acknowledgments

Appendix A. Supplementary data

Supplementary data associated with this article can be found, in the online version, at https://doi.org/10.1016/j.acthis.2018.02.010.

References

encan A, et al. 2004; Testis fixation in prepubertal rats: fibrin glue versus transparenchymal sutures reduces testicular damage. Eur J Pediatr Surg. 14 (03) :193–197. [PubMed: 15211411]

Ainslie KM, et al. 2009; In vitro inflammatory response of nanostructured titania: silicon oxide, and polycaprolactone. J Biomed Mater Res A. 91 (3) :647–655. [PubMed: 18988278]

Anderson JM. 2001; Biological responses to materials. Annu Rev Mater Res. 31 (1) :81–110.

Andrade MG, Weissman R, Reis SR. 2006; Tissue reaction and surface morphology of absorbable sutures after in vivo exposure. J Mater Sci. 17 (10) :949–961.

Ascherman J, Jones V, Knowles S. 2005; The histologic effects of retention sutures on wound healing in the rat. Wounds Compend Clin Res Pract. 17 (10) :271–277.

Badylak S, et al. 1998; Small intestinal submucosa: a rapidly resorbed bioscaffold for augmentation cystoplasty in a dog model. Tissue Eng. 4 (4) :379–387. [PubMed: 9916170]

Costa JNL, et al. 2005; Comparison between the decellularized bovine pericardium and the conventional bovine pericardium used in the manufacture of cardiac bioprostheses. Braz J Cardiovasc Surg. 20 (1) :14–22.

Cunniffe GM, et al. 2015; Porous decellularized tissue engineered hypertrophic cartilage as a scaffold for large bone defect healing. Acta Biomater. 23 :82–90. [PubMed: 26038199]

Giavaresi G, et al. 2006; In vitro and in vivo response to nanotopographically-modified surfaces of poly (3-*hydroxybutyrate*-co-3-*hydroxyvalerate*) and polycaprolactone. J Biomater Sci Polym Ed. 17 (12) :1405–1423. [PubMed: 17260511]

Gogolewski S, et al. 1993; Tissue response and in vivo degradation of selected polyhydroxyacids: polylactides (PLA), poly (3-*hydroxybutyrate*)(PHB), and poly (3-*hydroxybutyrate*-co-3-*hydroxyvalerate*)(PHB/VA). J Biomed Mater Res A. 27 (9) :1135–1148.

Guarnieri M, et al. 2014; Subcutaneous implants for long-acting drug therapy in laboratory animals may generate unintended drug reservoirs. J Pharm Bioallied Sci. 6 (1) :38. [PubMed: 24459402]

Hennessy RS, et al. 2017; Supercritical carbon dioxide–based sterilization of decellularized heart valves. JACC: Basic Transl Sci. 2 (1) :71–84. [PubMed: 28337488]

Katz S, Izhar M, Mirelman D. 1981; Bacterial adherence to surgical sutures: a possible factor in suture induced infection. Ann Surg. 194 (1) :35. [PubMed: 7018429]

Kim MS, et al. 2007; An in vivo study of the host tissue response to subcutaneous implantation of PLGA-and/or porcine small intestinal submucosa-based scaffolds. Biomaterials. 28 (34) :5137–5143. [PubMed: 17764737]

Lai PH, et al. 2005; Peritoneal regeneration induced by an acellular bovine pericardial patch in the repair of abdominal wall defects. J Surg Res. 127 (2) :85–92. [PubMed: 15921700]

Mazza G, et al. 2015; Decellularized human liver as a natural 3D-scaffold for liver bioengineering and transplantation. Sci Rep. 5 :13079. [PubMed: 26248878]

Meagher MJ, et al. 2016; Acellular hydroxyapatite-collagen scaffolds support angiogenesis and osteogenic gene expression in an ectopic murine model: effects of hydroxyapatite volume fraction. J Biomed Mater Res A. 104 (9) :2178–2188. [PubMed: 27112109]

Mirsadraee S, et al. 2007; Biocompatibility of acellular human pericardium. J Surg Res. 143 (2) :407–414. [PubMed: 17574597]

Modulevsky DJ, Cuerrier CM, Pelling AE. 2016; Biocompatibility of subcutaneously implanted plant-derived cellulose biomaterials. PLoS One. 11 (6) :e0157894. [PubMed: 27328066]

Neethling WM, Glancy R, Hodge AJ. 2010; Mitigation of calcification and cytotoxicity of a glutaraldehyde-preserved bovine pericardial matrix: improved bio-compatibility after extended implantation in the subcutaneous rat model. J Heart Valve Dis. 19 (6) :778. [PubMed: 21214104]

Nillesen ST, et al. 2007; Increased angiogenesis and blood vessel maturation in acellular collagen–heparin scaffolds containing both FGF2 and VEGF. Biomaterials. 28 (6) :1123–1131. [PubMed: 17113636]

Record RD, et al. 2001; In vivo degradation of 14 C-labeled small intestinal submucosa (SIS) when used for urinary bladder repair. Biomaterials. 22 (19) :2653–2659. [PubMed: 11519785]

Rennert RC, et al. 2013; Cellular response to a novel fetal acellular collagen matrix: implications for tissue regeneration. Int J Biomater. 2013

Ripamonti U. 1996; Osteoinduction in porous hydroxyapatite implanted in heterotopic sites of different animal models. Biomaterials. 17 (1) :31–35. [PubMed: 8962945]

Sarkanen JR, et al. 2012; Bioactive acellular implant induces angiogenesis and adipogenesis and sustained soft tissue restoration in vivo. Tissue Eng Part A. 18 (23–24) :2568–2580. [PubMed: 22738319]

Setzen G, Williams EF III. 1997; Tissue response to suture materials implanted subcutaneously in a rabbit model. Plast Reconstr Surg. 100 (7) :1788–1795. [PubMed: 9393477]

Singh S, Wu BM, Dunn JC. 2011; Accelerating vascularization in polycaprolactone scaffolds by endothelial progenitor cells. Tissue Eng Part A. 17 (13–14) :1819–1830. [PubMed: 21395445]

Stapleton TW, et al. 2010; Investigation of the regenerative capacity of an acellular porcine medial meniscus for tissue engineering applications. Tissue Eng Part A. 17 (1–2) :231–242. [PubMed: 20695759]

Sun H, et al. 2006; The in vivo degradation: absorption and excretion of PCL-based implant. Biomaterials. 27 (9) :1735–1740. [PubMed: 16198413]

Thiel M, et al. 2005; A stereological analysis of fibrosis and inflammatory reaction induced by four different synthetic slings. BJU Int. 95 (6) :833–837. [PubMed: 15794793]

Tran HLB, et al. 2016; Preparation and characterization of acellular porcine pericardium for cardiovascular surgery. Turk J Biol. 40 (6) :1243–1250.

Vogel B, et al. 2015; Determination of collagen content within picrosirius red stained paraffin-embedded tissue sections using fluorescence microscopy. MethodsX. 2 :124–134. [PubMed: 26150980]

Walles T, et al. 2003; Acellular scaffold implantation?no alternative to tissue engineering. Int J Artifi Org. 26 (3) :225–234.

Wang Z, et al. 2005; Evaluation of biodegradable synthetic scaffold coated on arterial prostheses implanted in rat subcutaneous tissue. Biomaterials. 26 (35) :7387–7401. [PubMed: 16019065]

Wang F, et al. 2017; Regeneration of subcutaneous tissue-engineered mandibular condyle in nude mice. J Cranio-Maxillofac Surg. 45 (6) :855–861.

Wu Q, et al. 2016; In vivo effects of human adipose-derived stem cells reseeding on acellular bovine pericardium in nude mice. Exp Biol Med. 241 (1) :31–39.

Yang Q, et al. 2008; A cartilage ECM-derived 3-D porous acellular matrix scaffold for in vivo cartilage tissue engineering with PKH26-labeled chondrogenic bone marrow-derived mesenchymal stem cells. Biomaterials. 29 (15) :2378–2387. [PubMed: 18313139]

Zhang J, et al. 2011; The biomechanical behavior and host response to porcine-derived small intestine submucosa: pericardium and dermal matrix acellular grafts in a rat abdominal defect model. Biomaterials. 32 (29) :7086–7095. [PubMed: 21741703]

Zheng MH, et al. 2005; Porcine small intestine submucosa (SIS) is not an acellular collagenous matrix and contains porcine DNA: possible implications in human implantation. J Biomed Mater Res B Appl Biomater. 73 (1) :61–67. [PubMed: 15736287]
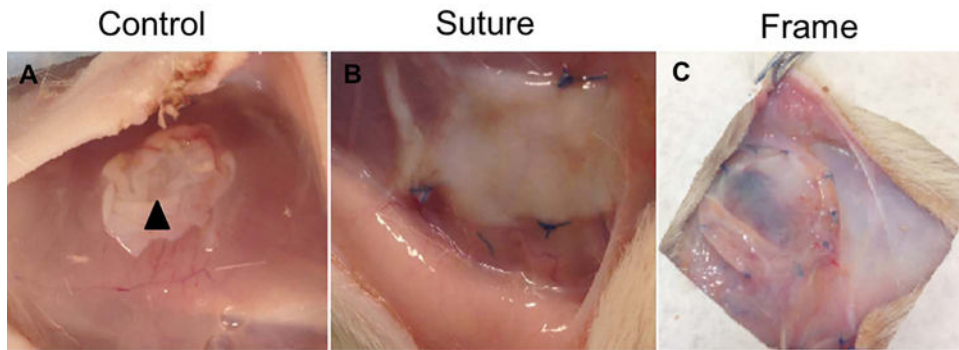
Fig. 1.
In vivo implantation of pericardial scaffolds including methods utilized. Decellularized and sterilized porcine pericardial scaffolds were cut into 20 mm × 20 mm segments and placed subcutaneously A) without suturing or fixation that showed scaffold folding and shrinkage after 4 weeks denoted with black arrow. B) over the muscle sutured at four corners with Polypropylene 5-0 that showed integration into the host within 1-week post-explant and degradation after 4 weeks, and C) fixed to a PCL rim frame by Polypropylene 5-0 under aseptic conditions, placed between skin and fascia, and left in position that showed no gross changes after 4 weeks.
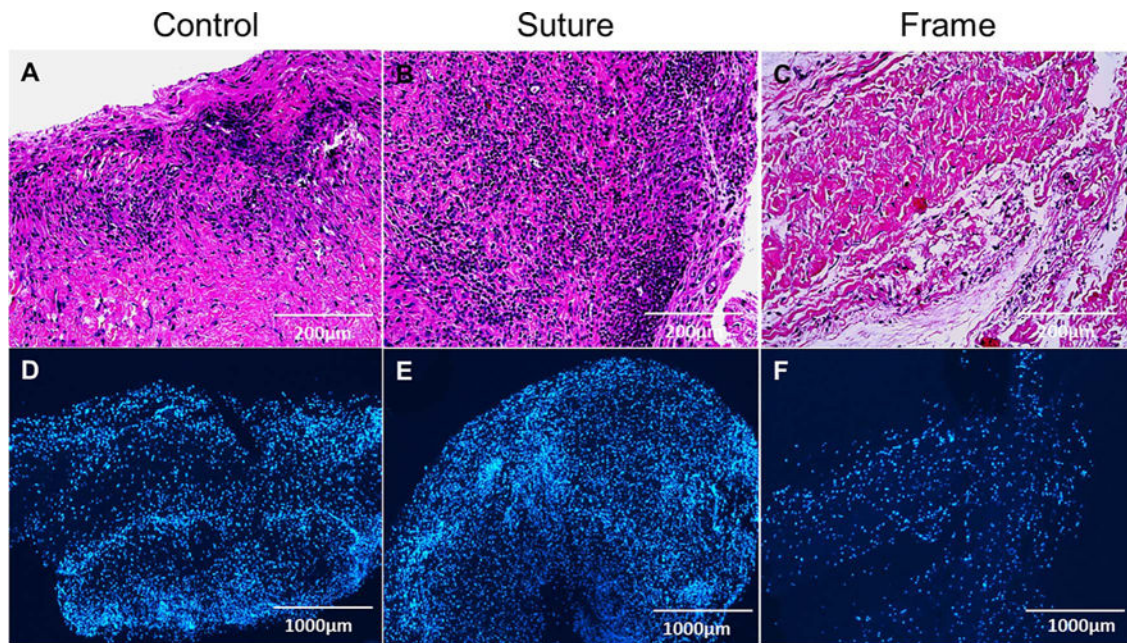
Fig. 2.
Hematoxylin & Eosin and DAPI stains showing cellularity and DNA content of pericardial scaffolds at 4 weeks. (A–C) H&E at 20 × showed increased cellular infiltration with indication of acute and chronic inflammatory cells in control and suture methods. Frame method showed progressive recellularization overtime. (D–F) DAPI at 4× magnification showed progressive recellularization for all methods, but increased infiltration in both control and suture methods.
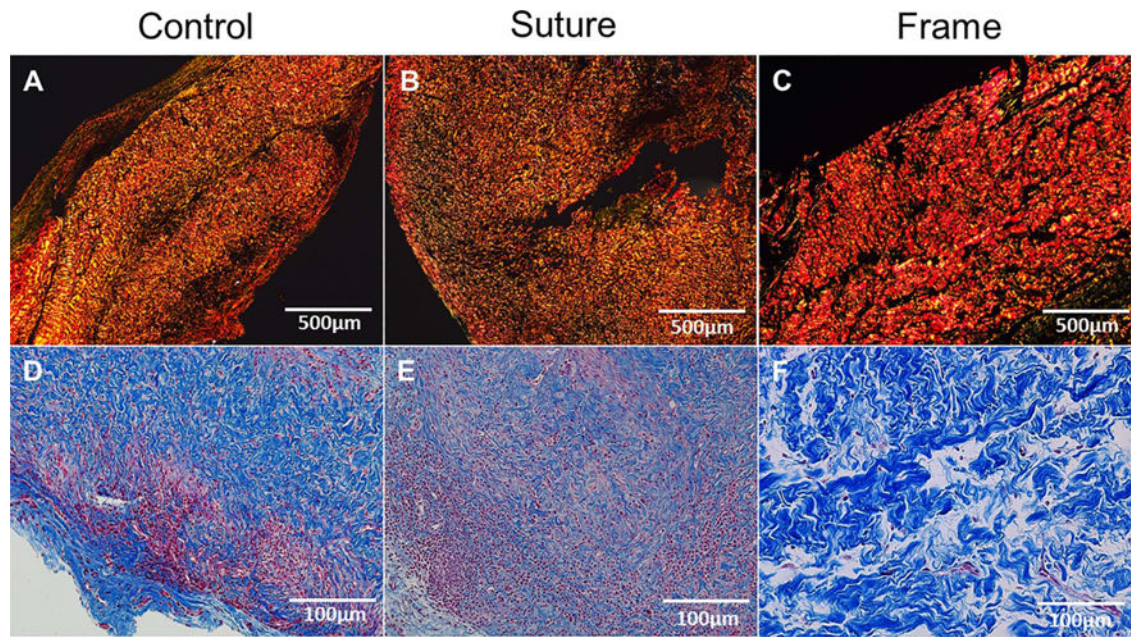
Fig. 3.
Collagen deposition. (A–C) Picrosirius staining showed decreased collagen content at 4 weeks. Comparison of collagen content between groups showed increased content in frame methods compared to suture and control methods. (D–F) Masson trichrome staining showed increased inflammatory cell in control and suture groups that invaded the collagenous structure. The frame method showed no evidence of inflammatory cells and intact collagen structure in frame method.
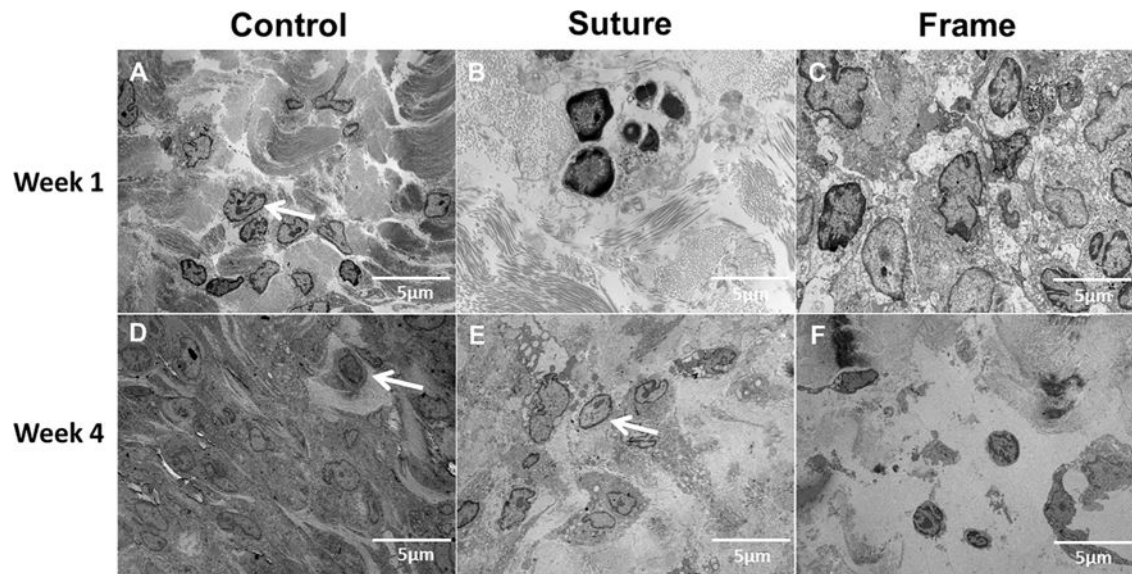
Fig. 4.
Transmission Electron Microscopy at Weeks 1 and 4. (A–F) TEM analysis showed presence of inflammatory cells composed of neutrophil and macrophages (white arrows). (A,D) Control method contained increased neutrophils post implantation. (E) Suture method showed presence of inflammatory cells at 4 weeks but not at 1 week, and (C,F)In the frame method, there were no inflammatory cells present.
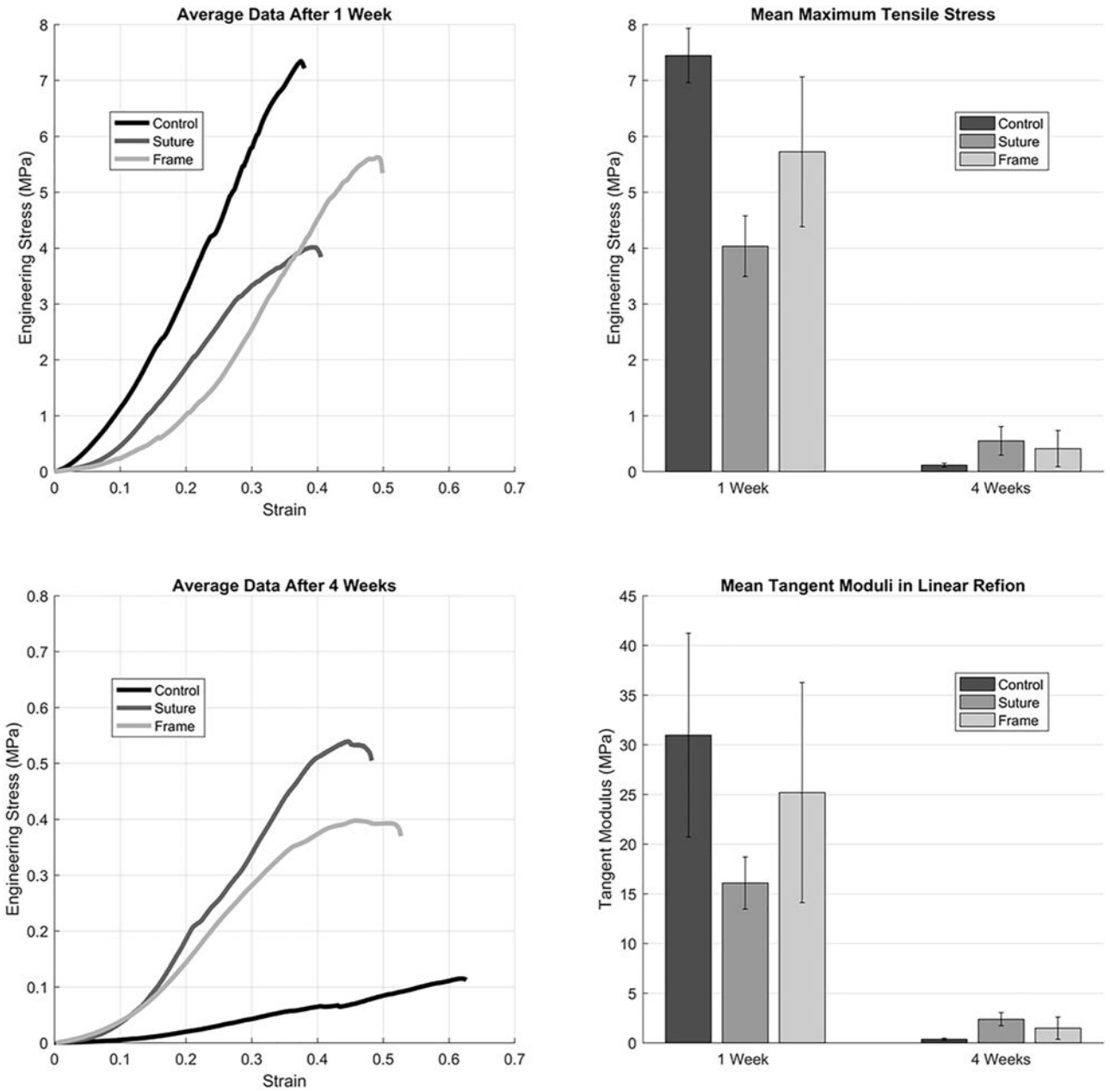
Fig. 5.
Uniaxial mechanical testing of 3-methods at all time points. The tensile stress test showed significant decrease from 1 to 4 weeks in all methods. The control method and frame method has more tensile stress in 1 weeks but the control methods tensile stress drop after 4 weeks. At 4 weeks the suture and frame methods has highest tensile test compared to control methods.
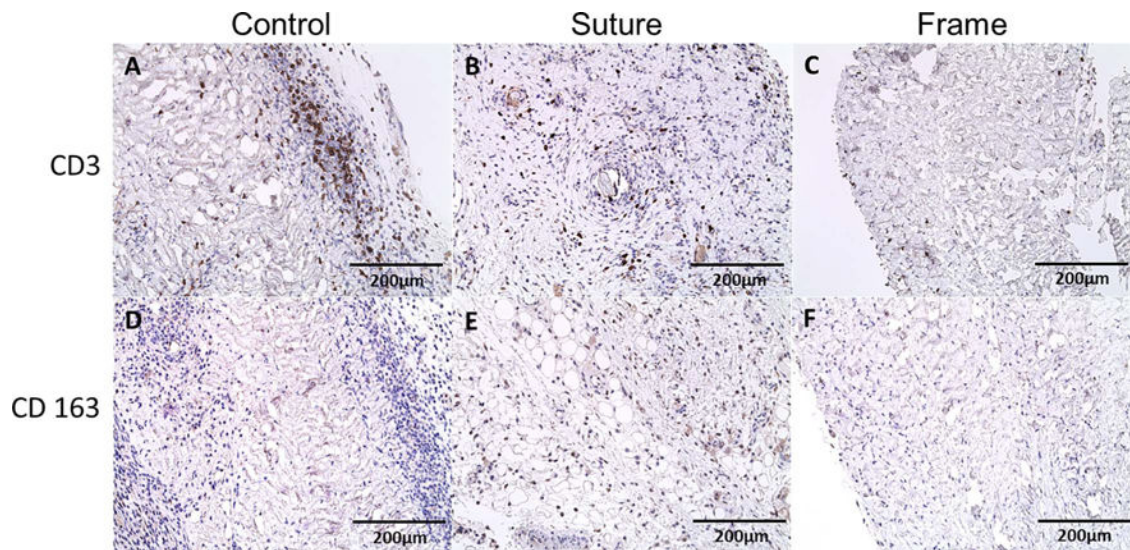
Fig. 6.
Immunohistochemistry of inflammation with CD3 and CD163 biomarkers after 1 Week
Post-Explantation. The CD 3 staining showed increase inflammatory cells in both the (A)
control and (B) suture methods compared to the (C) frame method. Specific staining for
macrophage type 2 utilizing CD 163 revealed very weak staining after 1 week in (D) control,
(E) suture, and (F) frame methods.
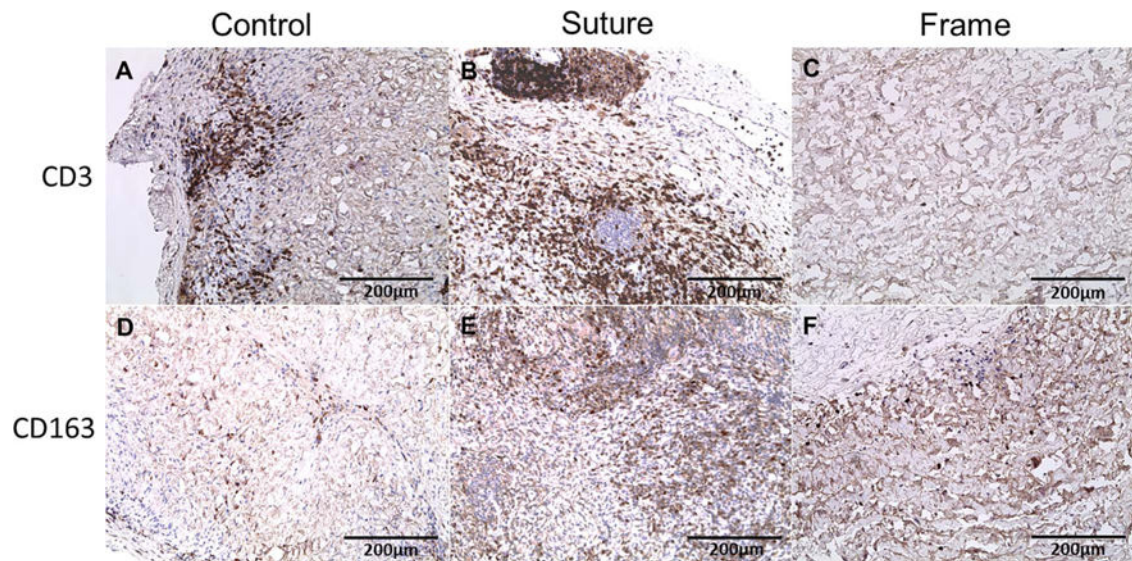
Fig. 7.
Immunohistochemistry of inflammation with CD3 and CD163 biomarkers. (A–B) Positive expression of the CD3 biomarker in both the control and suture methods after 4 weeks showing chronic inflammatory lymphocytes compared to (C) the frame method with no expression of CD3 suggesting no inflammation. CD 163 biomarker, specific for macrophage subtype II, showed a positive expression in (E) suture and (F) frame methods suggestive of increased regenerative capacity over time.
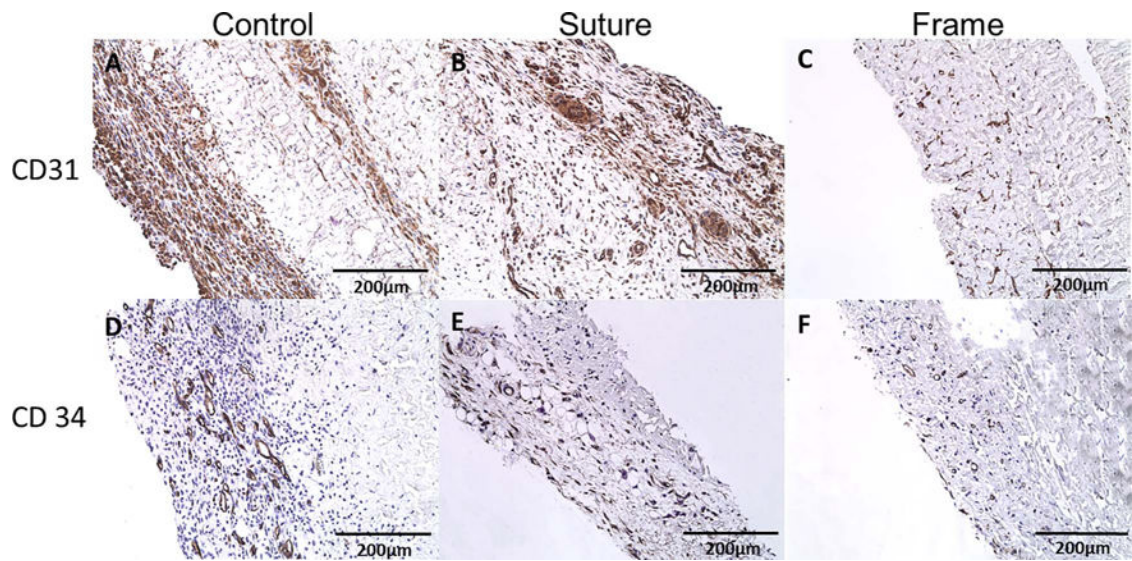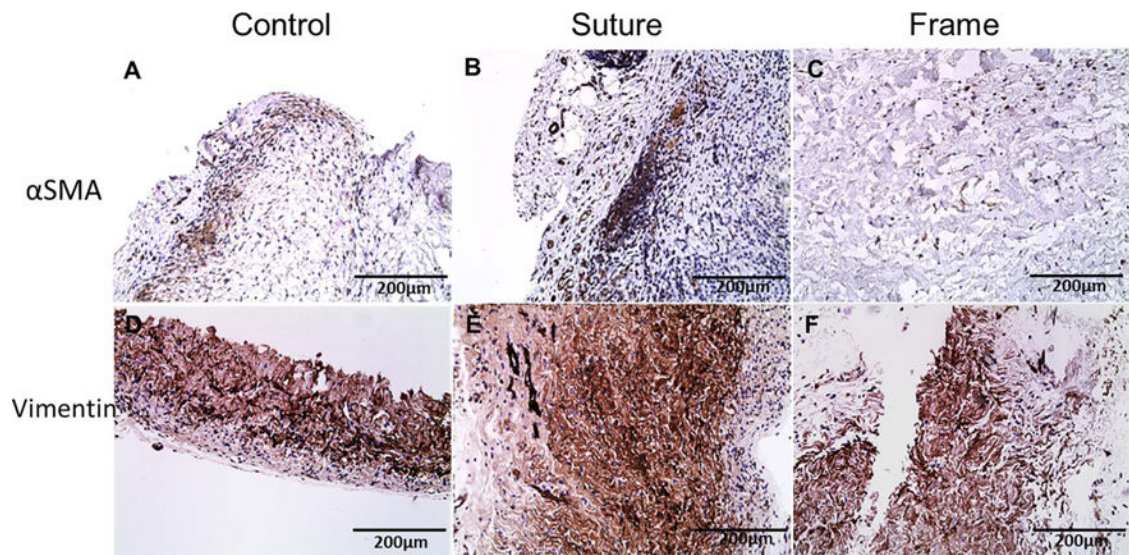
Fig. 8.

Immunohistochemistry of inflammation with CD31 and CD34 biomarkers after 1 Week Post-Explantation. Angiogenesis markers CD 31 and CD 34 showed highly positive staining in the (A,D) control and (B,E) suture methods.
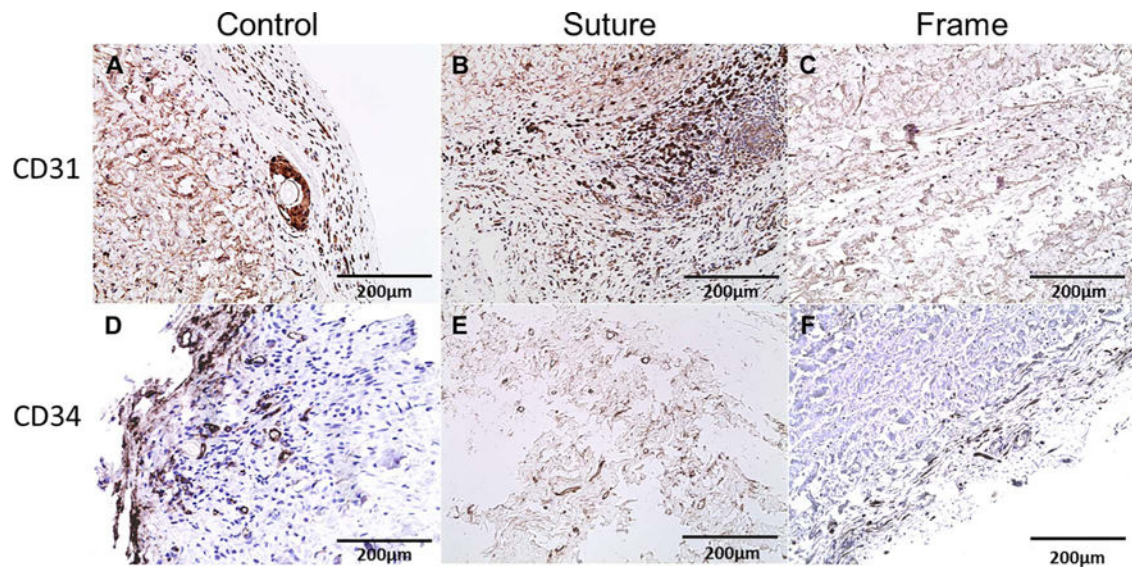
Fig. 9.
Immunohistochemistry of endothelial-like cells with CD31 and CD34 biomarkers at 4 weeks. (A–B) CD31 biomarkers showed a positive expression indicating endothelialization of neovasculature. C) Minimal expression of CD31 in frame method of implantation. (D–F) CD34 biomakers showing expression of angiogenesis in all three methods throughout the study duration.

Fig. 10.
Immunohistochemical staining of interstitial-like cells with Alpha-Smooth Muscle Actin and Vimentin biomarkers. Alpha Smooth muscle actin staining showed highly expressed level after 4 weeks in (A) control and (B) suture methods, which indicate presence of myofibroblast-like interstitial cell infiltration. Vimentin positive cells showed progressive increase 4 weeks in all methods (D–F).
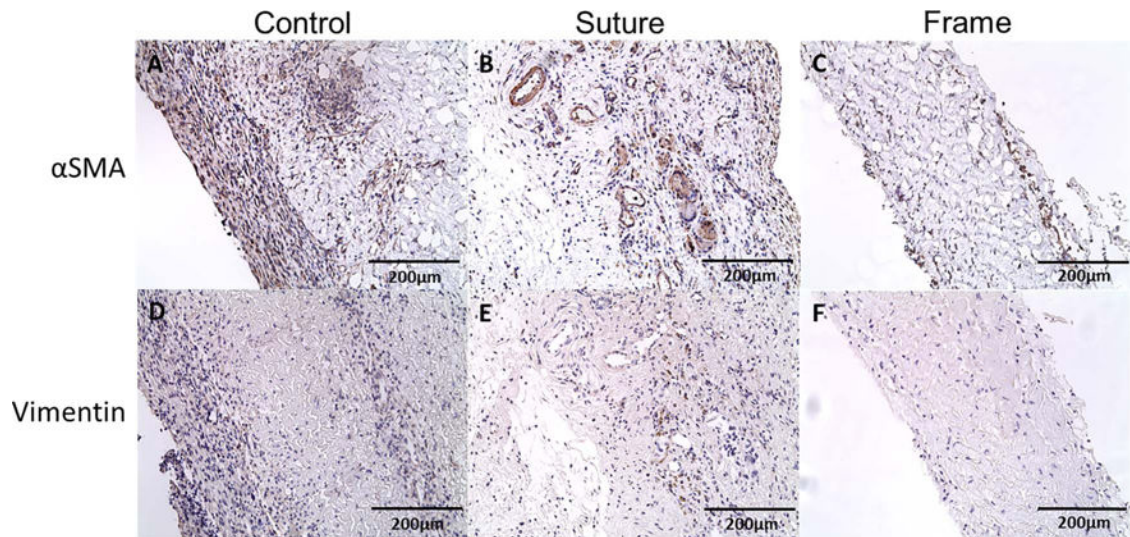
Fig. 11.
Immunohistochemistry of inflammation with Alpha-SMA and Vimentin biomarkers after 1 Week Post-Explantation. Alpha-SMA staining showed that there was moderate positive staining in (A) control and (B) suture methods; however, there was mild positive staining of the (C) frame method tissue. Vimentin staining showed mild positive staining in (D) control, (E) suture, and (F) frame methods at 1 week.

Table 1

Statistical comparisons of collagen content found from semi-quantative analysis of picrosirius red staining for each implantation method between implantation methods at each explant time. Significant values (p < 0.05) are shown with an asterisk.

	Comparison Between Groups at Week 1			Comparison Between Groups at Week 4		
	Control *vs* Suture	Control *vs* Frame	Suture *vs* Frame	Control *vs* Suture	Control *vs* Frame	Suture *vs* Frame
Collagen Content	0.3263	0.5119	0.9149	0.5019	0.6522	0.1697

Table 2

Statistical comparisons of fracture stress and tangent modulus between implantations methods at each explant time. Significant values (p < 0.05) are shown with an asterisk.

	Comparison Between Groups at Week 1			Comparison Between Groups at Week 4		
	Control *vs* Suture	Control *vs* Frame	Suture *vs* Frame	Control *vs* Suture	Control *vs* Frame	Suture *vs* Frame
Fracture Stress	0.0082*	0.1209	0.1134	0.2211	0.8078	0.3384
Tangent Modulus	0.1864	0.4404	0.7013	0.0872	0.4806	0.2660

Table 3

Statistical comparisons of various IHC semi-quantative analyses for each implantation method between implantation methods at each explant time. Significant values (p < 0.05) are shown with an asterisk.

Group Comp Week 1	Cd 3	Cd 31	Cd 34	Cd 163	αSMA	Vimentin
Control vs Suture	< 0.001*	< 0.001*	< 0.001*	< 0.001*	< 0.001*	0.2676
Control vs Frame	< 0.001*	< 0.001*	0.0023*	0.0072*	0.0011*	0.0029*
Suture vs Frame	< 0.001*	< 0.001*	< 0.001*	< 0.001*	< 0.001*	0.0541
Group Comp Week 4						
Control vs Suture	< 0.001*	< 0.001*	< 0.001*	< 0.001*	< 0.001*	0.5293
Control vs Frame	< 0.001*	< 0.001*	< 0.001*	0.0212*	< 0.001*	< 0.001*
Suture vs Frame	< 0.001*	0.0369*	< 0.001*	< 0.001*	< 0.001*	< 0.001*